

THE SHORT-RANGE TRANSVERSE WAKEFIELDS IN TESLA ACCELERATING STRUCTURE

I. Zagorodnov*, T. Weiland, Fachbereich 18, TU Darmstadt, 64287 Darmstadt, Germany

Abstract

The operation of a Free Electron Laser in TESLA project requires very short bunches. This results in a very long interaction length between the bunch and the wakefields. From this fact severe problems for computer simulations arise. The longitudinal case was recently studied intensively by Novokhatski et al.[1]. In this paper we study mainly the transverse forces. Using a recently developed time domain numerical approach, we calculate the short-range transverse wakefields of the TESLA linac accelerating structure. We also consider behaviour of transverse wake potential in a periodic array of cavities and compare it with wake potential of the TESLA quasi-periodic structure.

INTRODUCTION

For the operation of the Free Electron Laser in the TESLA project very short bunches of length $\sigma = 50$ micrometers or less are required. This bunch length is very short compared to the iris radius a of the accelerating structure ($\sigma/a \sim 0.0014$). This induces severe problems for computer simulations. The longitudinal case was recently studied intensively by Novokhatski et al. [1]. It was shown that as for periodic structures and very short bunches the loss factor becomes independent of the bunch length. In this paper we study mainly the transverse forces. Using a recently developed time domain numerical approach [2], we calculate the short-range transverse wakefields in the TESLA accelerating structure of three cryomodules with total length ~ 36 m. Wakefields in the TESLA cryomodule and corresponding integral parameters are given for bunches of different length. We also consider behaviour of transverse wake potential in a periodic array of cavities and compare it with wake potential of the TESLA quasi-periodic structure. The numerical results are compared with analytical estimations and it is shown that, the same as for periodic structure [3], for very short bunches the kick factor decreases linear with the bunch length.

ANALYTICAL ESTIMATIONS

We consider an axially symmetric structures and bunch with charge Q moving parallel to the axis. The bunch with longitudinal distribution $q(s)$ travels near the axis, and thus the longitudinal loss is dominated by monopole fields

$$L_{\parallel} \equiv \langle W_{\parallel}^0 \rangle = \frac{1}{Q} \int_{-\infty}^{\infty} W_{\parallel}^0(s) q(s) ds = \frac{1}{Q^2} \int_{-\infty}^{\infty} \int_{-\infty}^s w_{\parallel}^0(s-s') q(s') q(s) ds' ds$$

* Work supported in part by the Deutsche Forschungsgemeinschaft, project 1239/22-1

and the transversal kick by dipole fields

$$L_{\perp} \equiv \langle W_{\perp}^1 \rangle = \frac{1}{Q} \int_{-\infty}^{\infty} W_{\perp}^1(s) q(s) ds = \frac{1}{Q^2} \int_{-\infty}^{\infty} \int_{-\infty}^s w_{\perp}^1(s-s') q(s') q(s) ds' ds.$$

Short bunches interact with single cavity and periodical structure in a different way. However, in both cases the wake functions $w_{\parallel}^0(s)$ and $w_{\perp}^1(s)$ at short distance s are approximately related in the simple way [4]

$$w_{\perp}^1(s) \cong \frac{2}{a^2} \int_0^s w_{\parallel}^0(z) dz. \quad (1)$$

For short bunches in a single cavity the well known result of K. Bane and M. Sands [5] reads as

$$w_{\parallel}(s) = \frac{Z_0 c}{\sqrt{2\pi^2} a} \sqrt{\frac{g}{s}}, \quad w_{\perp}(s) = \frac{2}{a^2} \frac{\sqrt{2} Z_0 c}{\pi^2 a} \sqrt{g s}, \quad (2)$$

where a is the iris radius and g is the cavity gap. As we see relation (1) holds for the wakes (2).

In the periodic structure the short range wake functions can be approximated by the relations [4]

$$w_{\parallel}(s) = A \frac{Z_0 c}{\pi^2 a} \exp(-\sqrt{s/s_0}), \quad (3)$$

$$w_{\perp}(s) = \frac{2}{a^2} A \frac{Z_0 c}{\pi^2 a} 2s_1 \left(1 - \left(1 + \sqrt{s/s_1} \right) \exp(-\sqrt{s/s_1}) \right), \quad (4)$$

where A, s_0, s_1 are fit parameters to be defined. If $s_0 = s_1$ then relation (1) holds exactly. However, in the common case $s_0 \neq s_1$ we have only

$$\partial_s w_{\perp}^1(0) = \frac{2}{a^2} w_{\parallel}^0(0). \quad (5)$$

This corresponds to a small difference of the right hand and left- hand sides in (1) for short distances s .

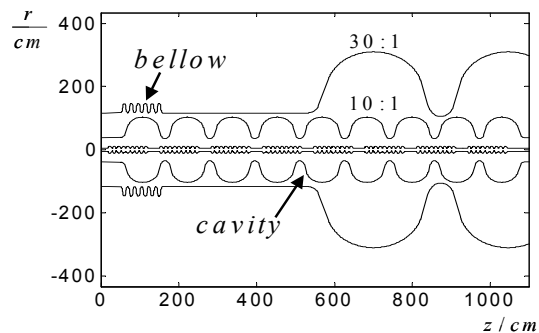


Fig. 1: Geometry of the TESLA cryomodule.

The TESLA linac consists of a long chain of cryomodules. One cryomodule of total length 12 m contains 8 cavities and 9 bellows as shown in Fig.1. The iris radius is 35 mm and beam tubes radius is 39 mm.

The wakefields for Gaussian bunches up to $\sigma = 50 \mu\text{m}$ are studied. To reach steady state solution the structure of 3 cryomodules with total length 36m considered.

SINGLE-CELL STRUCTURE

As the first step we study wake fields in one middle cell of 9-cell TESLA cavity with aperture $a = 35\text{mm}$. From the fit of numerical data to formulas (2) we obtain

$$w_{\parallel}(s) = \frac{Z_0 c}{\sqrt{2\pi^2 a}} \sqrt{\frac{\bar{g}}{s}} = 0.072 s^{-0.5} [\text{V/pC}],$$

$$w_{\perp}(s) = \frac{2}{a^2} \frac{\sqrt{2} Z_0 c}{\pi^2 a} \sqrt{\bar{g} s} = 235 s^{0.5} [\text{V/pC/m}],$$

where \bar{g} is “effective” cavity gap, $\bar{g} = 0.84L$, expressed through the cell period $L = 10.54\text{cm}$ in the TESLA cavity. As we see relation (1) holds exactly.

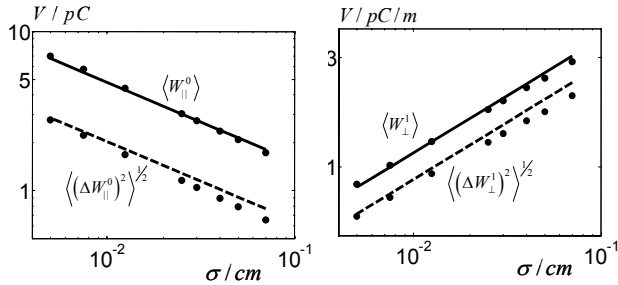


Fig. 2: Comparison of numerical and analytical integral parameters for a TESLA single-cell structure.

Fig.2 (left) shows the analytical (solid line) and numerical (points) loss factors and energy spreads (dashed line and points). On the right side of the figure the transversal kick and kick spread are shown. As we see the longitudinal loss factor scales as $O(\sigma^{-0.5}), \sigma \rightarrow 0$, and transversal kick factor scales as $O(\sigma^{0.5}), \sigma \rightarrow 0$.

PERIODIC STRUCTURE

In the case of a periodic structure the induced by short bunches wake fields can not be simply calculated as the sum of the single cell contributions, because the field traveling with the bunch is strongly modified and reach the steady state solution only after $\sim N = 2a^2 / (\sigma L)$ cells. To study the steady state solution in the periodic structure we calculate wake fields in the chain of 144 cells.

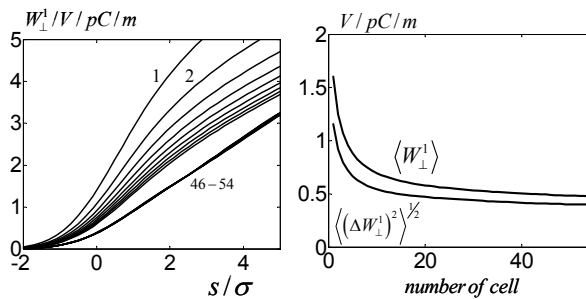


Fig. 3: Modification of the transverse wake potentials and the kick factor in periodic structure.

Fig. 3. shows the transverse wake potentials in the first nine cells (left) and the kick factor per cell for bunch with

$\sigma = 200\mu\text{m}$ (right) as a function of the number of cells. The kick factor converges to the steady state value.

From the fit of numerical data to formulas (3), (4) we obtain with $A = 1.025$, $a = 35\text{mm}$, wake functions per cell period $L = 10.54 [\text{cm/cell}]$

$$w_{\parallel}(s) = 3.47 \exp(-\sqrt{s/s_0}) [\text{V/pC/cell}],$$

$$w_{\perp}(s) = 15.64 \left[1 - \left(1 + \sqrt{\frac{s}{s_1}} \right) \exp\left(-\sqrt{\frac{s}{s_1}}\right) \right] \left[\frac{\text{V}}{\text{pC} \times \text{m} \times \text{cell}} \right],$$

where $s_0 = 3.46 \cdot 10^{-3}$ and $s_1 = 1.4 \cdot 10^{-3}$. Thus, for $s_0 \neq s_1$ relation (1) is not fulfilled exactly but relation (5) holds.

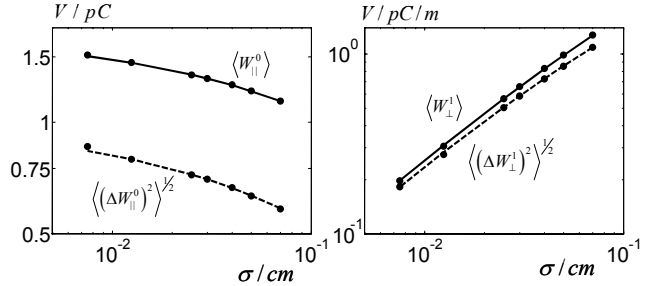


Fig. 4: Comparison of numerical and analytical integral parameters for periodic structure.

Fig. 4(left) shows the analytical (solid line) and numerical (points) loss factors and energy spreads (dashed line and points) for cell number 144. On the right side of the figure the transversal kick and kick spread are shown. As we see in the periodic case longitudinal loss factor becomes independent from the bunch length and transversal kick factor scales as $O(\sigma), \sigma \rightarrow 0$.

TESLA ACCELERATING STRUCTURE

The TESLA linac can be considered as multi-periodic structure: the first elementary period is the cavity cell, the second one is the 9-cell cavity with bellow and beam tubes and the third one is the cryomodule, housing 8 cavities with 9 bellows. In addition, some extra effects, like the larger tube diameter with respect to the aperture and different form of end cells of the cavity have to be taken into account. To reach steady state solution we calculate wake fields in the chain of 3 cryomodules.

From the fit of the numerical data to formulas (3), (4) we obtain with $A = 1.46$ and active length of cryomodule $L_a = 8 \cdot 1.036 [\text{m/module}]$ the wake functions per cryomodule

$$w_{\parallel}(s) = 344 \exp(-\sqrt{s/s_0}) [\text{V/pC/module}],$$

$$w_{\perp}(s) = 10^3 \left[1 - \left(1 + \sqrt{\frac{s}{s_1}} \right) \exp\left(-\sqrt{\frac{s}{s_1}}\right) \right] \left[\frac{\text{V}}{\text{pC} \times \text{m} \times \text{module}} \right],$$

where $s_0 = 1.74 \cdot 10^{-3}$ and $s_1 = 0.92 \cdot 10^{-3}$. In formulas (3), (4) we used “effective” iris radius $a = \bar{a} = 35.57\text{mm}$. It was chosen as value between the pipe and iris radii to fulfill relation (5) for the above given wake functions. Thus, for $s_0 \neq s_1$ relation (1) is not fulfilled exactly but

relation (5) holds again (with $a = \bar{a}$). Like in the periodic case the transversal wake function scales as $O(s), s \rightarrow 0$.

To obtain the formulas for the wake function on the unit of active length the above relations should be divided by $L_a = 8.288$ [m/module].

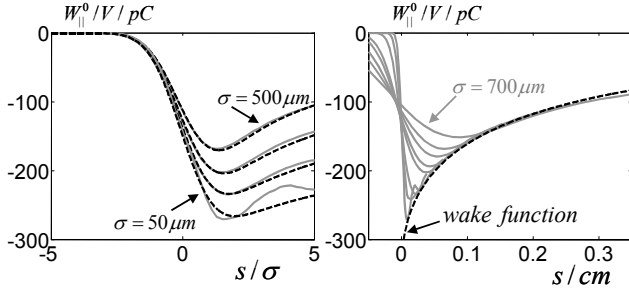


Fig. 5: Comparison of analytical and numerical longitudinal wakes in the third cryomodule ($\sigma = 50 \div 700\mu\text{m}$).

Fig. 5 (left) shows numerical (gray solid lines) and analytical (black dashed lines) wake potentials for bunches with $\sigma = 50, 250, 125, 50\mu\text{m}$. The deviation of the curves for the shortest bunch can be explained by the insufficiency of the 3 cryomodules to reach the steady-state solution. Fig. 5 (right) shows the wakes (gray lines) together with the analytical wake function (black dashed line) which tends to be the envelope function to all wakes.

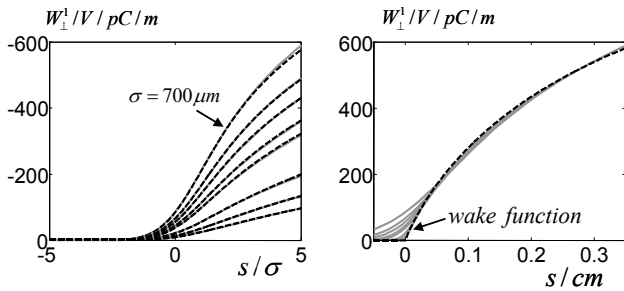


Fig. 6: Comparison of analytical and numerical transversal wake potentials in the third cryomodule ($\sigma = 50 \div 700\mu\text{m}$).

Fig. 6 shows likewise the results for transversal wakes. Again, the analytical wake function (black dashed line) tends to be the envelope function to all wakes (see Fig.6 right).

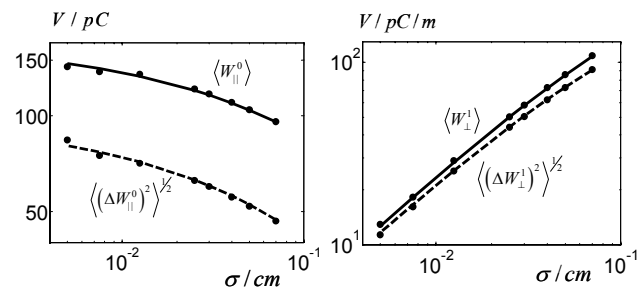


Fig. 7: Comparison of numerical and analytical integral parameters for the third TESLA cryomodule.

Fig. 7 (left) shows the analytical (solid line) and

numerical (points) loss factors and energy spreads (dashed line and points) in the third TESLA cryomodule. On the right side of the figure transversal kick and kick spread are shown.

Table 1. Comparison of the numerical and analytical loss factors.

$\sigma / \mu\text{m}$	Loss factor/V/pC		
	Numerical	Analytical	TDR
1000	86.4	90.2	90.4
700	95.9	95.8	95.6
500	105	104	103
400	110	110	108
300	117	116	114
250	122	120	117
125	135	133	128
75	138	141	134
50	143	146	138

Table 2. Comparison of the numerical and analytical kick factors.

$\sigma / \mu\text{m}$	Kick factor/V/pC/m		
	Numerical	Analytical	TDR
1000	138	137	153
700	109	108	130
500	85.4	85.1	111
400	72.5	72.2	99.6
300	58.1	57.9	86.8
250	50.2	50.1	79.6
125	28.8	28.3	56.9
75	18.2	18.1	44.3
50	12.8	12.6	36.3

Finally, in Tables 1,2 we compare numerical values with analytical ones obtained from the above formulas (“analytical”) and the formulas given in [6] (“TDR”). As we see for the longitudinal case the results agree inside of the 5% level. For the transversal case the TDR formula

$$w_{\perp}(s) = L_a \left(1290\sqrt{s} - 2600s \right) \left[\frac{V}{\text{pC} \times \text{m} \times \text{module}} \right]$$

shows for the short bunches wrong $O(s^{0.5}), s \rightarrow 0$, behavior and overestimates the kicks.

ACKNOWLEDGEMENTS

The authors thank K. Bane and M. Dohlus for helpful discussions.

REFERENCES

- [1] Novokhatski A., Timm M., Weiland T., DESY TESLA-99-16, 1999.
- [2] Zagorodnov I., Weiland T., Proc. of ICAP 2002.
- [3] Fedotov A.V., Gluckstern R.L., Venturini M., Phys. Rev. STAB, Vol.2, 064401, 1999.
- [4] Bane K.L.F., SLAC-PUB-9663, LCC-0116, 2003.
- [5] Bane K., Sands M., SLAC-PUB-4441, 1987.
- [6] TESLA Technical Design Report, DESY 2001-011.